ACS APPLIED MATERIALS & INTERFACES

Research Article

www.acsami.org

Innovative TiO_2/Cu Nanosurfaces Inactivating Bacteria in the Minute Range under Low-Intensity Actinic Light

O. Baghriche,[†] S. Rtimi,[†] C. Pulgarin,*[,†] R. Sanjines,[‡] and J. Kiwi*[,§]

[†]EPFL-SB-ISIC-GPAO, Ecole Polytechnique Fédérale de Lausanne, Station 6, CH-1015, Lausanne, Switzerland

[‡]EPFL-SB-IPMC-LNNME, Ecole Polytechnique Fédérale de Lausanne, Bat PH, Station 3, CH-1015, Lausanne, Switzerland

[§]EPFL-SB-ISIC-LPI, Ecole Polytechnique Fédérale de Lausanne, Bat Chimie, Station 6, CH-1015, Lausanne, Switzerland

ABSTRACT: The bacterial inactivation of *E. coli* by cotton TiO_2/Cu DC-magnetron sputtered thin films was investigated in the dark and under low-intensity actinic light. The TiO_2/Cu sputtered layers revealed to be sensitive to actinic light showing the spectral characteristics of Cu/CuO. This indicates that Cu does not substitute Ti^{4+} in the crystal lattice. Under diffuse actinic light (4 mW/cm^2), the hybrid composite TiO_2/Cu sample lead to fast bacterial inactivation times <5 min. This study presents evidence for a direct relation between the film optical absorption obtained by diffuse reflectance spectroscopy (DRS) and the bacterial inactivation kinetics by the TiO_2/Cu samples. The Cu-ions inactivating the bacteria were followed in solution by inductively plasma coupled spectroscopy (ICPS). The amounts of Cu-ions detected by ICPS provide the evidence for an oligodynamic antibacterial effect. The changes in the oxidation state of Cu during bacterial inactivation were followed by XPS. The *E. coli* cell viability was detected by standard coliform counting CFU methods. The TiO_2/Cu thickness layer was determined by profilometry and the film microstructure by XPS, TEM, AFM, XRD, XRF and contact angle (CA). A mechanism of bacterial inactivation by TiO_2/Cu samples is suggested in terms of interfacial charge transfer (IFCT) involving charge transfer between TiO_2 and Cu.

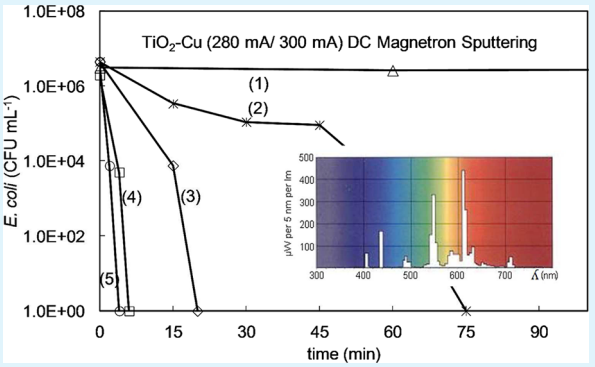

KEYWORDS: *bacterial inactivation, DC-sputtering, Cu/TiO_2 nanoparticulate films, oligodynamic effect*

INTRODUCTION

Antimicrobial surfaces are interesting because they can reduce or eliminate hospital-acquired infections (HAI) due to antibiotic resistant bacteria that survive on hospital surfaces for long times.[1,2] Cu-bactericide properties have been known for decades due to the release of small amounts of metal ions into the tissues/fabrics/diverse surfaces[3] avoiding the use of antiseptics/antibiotics after use.[4,5] The particular interest in Cu-textiles is based on the fact that the humid porous hydrophilic structure of textiles provides a suitable environment for bacterial growth. Cu sputtering has shown to improve the antibacterial properties of textile substrates. Gabbay et al.[6,7] has reported the technology to introduce Cu into natural and artificial fibers to preclude viral transmission, nosocomial infections and antibiotic resistant bacteria. In recent years, physical vapor deposition (PVD) has evolved to more performing sputtering chambers to modify the structure of fibers to produce antimicrobial surfaces.[8,9]

This study addresses the bacterial inactivation of cotton DC-sputtered surfaces of TiO_2, Cu and TiO_2/Cu illuminated with low intensity visible/actinic light. This approach is a different to the one used by Hashimoto et al[10] who prepared the TiO_2/Cu thin films by dip-coating cell technique and UV-irradiated the samples to induce bacterial inactivation. Later, the same group added Cu to extend TiO_2 absorption in to the visible range. Cu also may act as a trap for charge carriers to avoid charge recombination with TiO_2.[11,12]

Furthermore, Heidenau et al.[13,14] have recently demonstrated that Cu induces bacterial cell toxicity without decreasing significantly the cell biocompatibility. Cu was shown to be effective against *S. aureus ATTC 25923* retaining excellent cytocompatibility. The motivation to focus this study on Cu-supported cotton relates to recent work in our laboratory showing fast kinetic bacterial inactivation.[15−21] No mechanism for the interaction of TiO_2/Cu with *E. coli* will be presented in this study. But the most relevant mechanistic features based will be briefly addressed. The mechanistic features of *E. coli* inactivation by TiO_2 under light have been reported.[22−25]

The objective of this study is to prepare, evaluate and optimize the microstructure of TiO_2/Cu nanoparticulate sputtered on cotton inactivating *E. coli*. The Cu-ionic species released by the samples will be followed by Inductively Coupled Plasma Mass spectrometry (ICP-MS). The hydrophobic/hydrophilic balance and rugosity, the thickness, the Cu particle size, and the optical absorption will be reported for the TiO_2/Cu cotton inducing fast bacterial inactivation.

Received: June 25, 2012
Accepted: August 30, 2012
Published: September 28, 2012

EXPERIMENTAL SECTION

Sputtering of Cotton Samples, Profilometry. The TiO_2 was sputtered from a Ti-target (Lesker Ltd., UK) 2 in. diameter at 280 mA and applying a bias voltage of 406 V (106 W) in a (P_{Ar} + P_{O2}) atmosphere with an O_2 partial pressure 0.08 Pa and a total pressure of P = 0.4. The glow discharge plasma was generated in front of the Ti-target as recently reported for DC-deposition.[17] Cu was sputtered at 300 mA applying a bias voltage of 622 V (255W). We obtained sufficient adhesion of Cu to the cotton from Cilander AG, Herisau, CH-1109 Switzerland, and friction with paper or cloth did not lead to smearing of the Cu. This is an improvement with respect to the adhesion of Cu-particle fixed on RF-plasma textiles from CuO suspensions.[16] Deposition times up to 150s for TiO_2 and for Cu lead to the thicknesses shown in Figure 1.

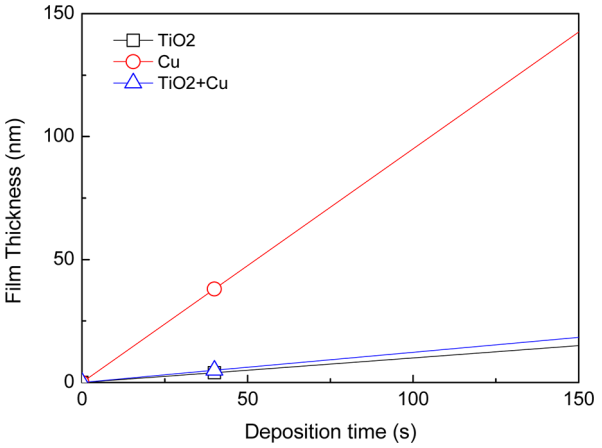

Figure 1. Calibration of the TiO_2, Cu, and TiO_2 + Cu thickness DC-sputtered on Si wafers.

Figure 1 shows that sputtering TiO_2 for 10 min lead to a film thickness of 60 nm ± 5%. Because one atomic layer contains about 1 × 10^{15} atoms/cm^2 and is ~0.2 nm thick,[8,9] a coating 60 nm thick is equivalent to ~300 layers. The TiO_2 deposition rate was of 2 × 10^{15} atoms/cm^{2}s. Sputtering for 40s Cu led to a coating of 38 nm ±5%. Figure 1 shows that within 1000 s, a Cu thickness of 900 nm was attained. This allows the estimation of the Cu-sputtering rate at 4.5 × 10^{15} atoms/cm^{2}s.

Sputtering both TiO_2 for 10 min and with Cu for 40s led to films 78 nm instead of a 98 nm thick composite layer as expected from the addition of the TiO_2 and Cu-layers. This suggests the formation of composite film made up of TiO_2/Cu. The film thickness was determined with a profilometer (Alphastep500, TENCOR).

The sputtering was carried out on square 2 × 2 cm cotton samples. Experiments to evaluate bacterial inactivation used one sample and the experimental data reporting bacterial inactivation in Figures 2, 4, and 5 were run in triplicate.

X-ray Fluorescence (XRF). The TiO_2 and Cu content on the cotton were evaluated by X-ray fluorescence. By this technique, each element emits an X-ray of a certain wavelength associated with its particular atomic number. The spectrometer used was RFX, PANalytical PW2400. TiO_2 DC-sputtering at 280 mA for times of 1,2,4,6,8 and 10 min lead to TiO_2 of 0.134, 0.362, 0431, 0.565, 0.655, and 0.686 wt %/wt cotton, respectively. Cu sputtering at 300 mA for times 10, 20, 40 and 60 s led to 0.160, 0.230, 0.329, and 0.348 wt %/wt cotton. Table 1 presents the composition for TiO_2/Cu films. It is readily seen that for 40s Cu-sputtering, a higher TiO_2 content in the underlying layers lead to samples with a lower % Cu wt/wt in the topmost layers.

Bacterial Inactivation and Sample Irradiation Procedures. Samples of *Escherichia coli* (*E. coli* K12) was obtained from the Deutsche Sammlung von Mikroorganismen and Zellkulturen GmbH (DSMZ) ATCC23716, Braunschweig, Germany, to test bacterial

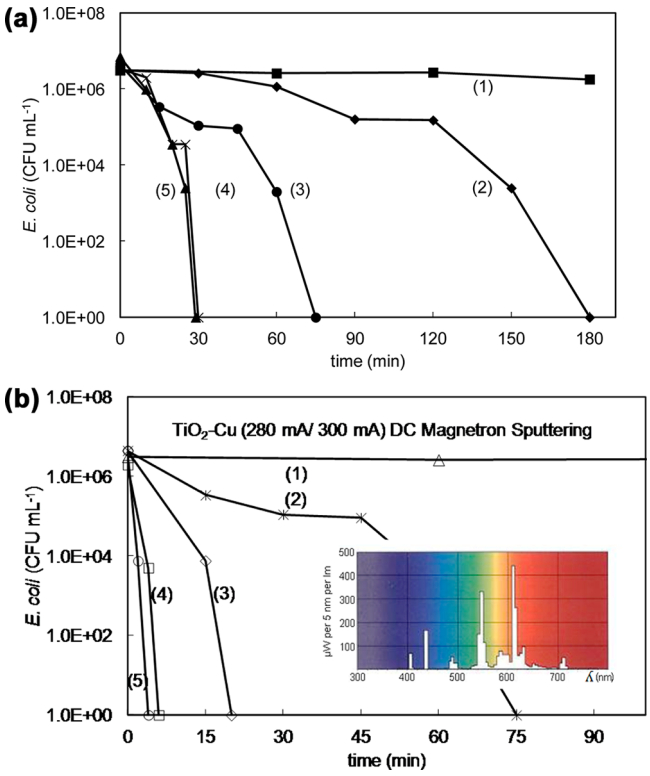

Figure 2. (a) Bacterial inactivation kinetics in the dark for samples: (1) cotton alone, (2) cotton-sputtered TiO_2/Cu (10 min/10 s), (3) cotton-sputtered TiO_2/Cu (10 min/20 s), (4) cotton-sputtered TiO_2/Cu (10 min/40 s), (5) cotton-sputtered TiO_2/Cu (10 min/60 s). TiO_2 is sputtered first on cotton followed by Cu for the duration indicated in the captions. (b) Bacterial inactivation kinetics for samples under low-intensity actinic light 4.0 mW/cm^2 from a Lumilux Osram 18W/827 lamp: (1) cotton alone, (2) cotton-sputtered TiO_2 /Cu (10 min/10s) (3) cotton-sputtered TiO/Cu (10 min/20 s), (4) cotton-sputtered TiO_2/Cu (10 min/40 s) and (5) cotton-sputtered TiO_2/Cu (10 min/60 s). TiO_2 is sputtered first on cotton followed by Cu for the duration indicated in the captions.

Table 1. Composition of Sputtered Cotton Films Determined by X-ray Fluorescence (XRF)

sample cotton TiO_2/Cu	time Cu (s)	% TiO_2 wt/wt cotton	% Cu wt/wt cotton
TiO_2 (1 min)	10	0.115	0.102
	20	0.097	0.130
	40	0.096	0.305

inactivation. The cotton fabrics were sterilized by autoclaving at 121 °C for 2 h. The 20 μL aliquots of the cultures with an initial concentration of 3.8 × 10^6 CFU mL^{-1} in NaCl/KCl (pH 7) were placed on the coated cotton and uncoated (control) cotton samples. The samples were placed on Petri dish provided with a lid to prevent evaporation. After each determination, the fabric was transferred into a sterile 2 mL Eppendorf tube containing 1 mL of autoclaved NaCl/KCl saline solution. This solution was subsequently mixed thoroughly using a Vortex for 3 min. Serial dilutions were made in NaCl/KCl solution. A 100 μL sample of each dilution was pipetted onto a nutrient agar plate and then spread over the surface of the plate using standard plate method. Agar plates were incubated lid down, at 37 °C for 24 h, before colonies were counted. The bacteria inactivation results reported in Figures 2−4 were performed in triplicate. Data is expressed as a mean ± standard deviation.

To verify that no regrowth of *E. coli* occurs after the total inactivation observed in the first disinfection cycle, the film is

dx.doi.org/10.1021/am301153j | ACS Appl. Mater. Interfaces 2012, 4, 5234−5240

incubated for 24 h at 37 °C. Then bacterial suspension of 100 μL is deposited on three Petri dishes to obtain replicates of the bacterial counting. These samples were incubated at 37 °C for 24 h. No bacterial regrowth was observed.

Irradiation of the cotton samples was carried in a cavity by Osram Lumilux 18W/827 actinic lamps, with emission between 400 and 700 nm with an integral output of 1.1 mW/cm^2 resembling the solar light spectrum.

Diffuse Reflectance Spectroscopy of Sputtered Samples (DRS). Diffuse reflectance spectroscopy was carried out using a Perkin-Elmer Lambda 900 UV−vis−NIR spectrometer provided for with a PELA-1000 accessory within the wavelength range of 200−800 nm and a resolution of one nm. The Kubelka-Munk relations measuring K/S for cotton showing a nonuniform surface were used to convert reflectance measurements (R) into the equivalent absorption spectra. K and S are the absorption and scattering coefficients of TiO_2. The reflectance of MgO was used as reference (R_{MgO}). The absorption of the samples was plotted in Kubelka−Munk (KM) arbitrary units vs wavelength.

Transmission Electron Microscopy Results (TEM). The transmission electron microscopy was determined with a Philips CM-12 (field emission gun, 300 kV, 0.17 nm resolution) microscope at 120 kV to determine the grain size composition of the TiO_2 and TiO_2/Cu films. The cotton embedded in epoxy resin 45359 Fluka and the fabrics were cross-sectioned with an ultramicrotome (Ultracut E). Images were taken in Bright Field (BF) mode. EDS was used to determine surface element composition at the current beam position based on the property that the atoms of each element emit X-rays with a specific energy.

X-ray Photoelectron Spectroscopy of Samples (XPS). XPS of sputtered cotton samples was determined using an AXIS NOVA photoelectron spectrometer (Kratos Analytical, Manchester, UK) equipped with monochromatic AlKα ($h\nu$ = 1486.6 eV) anode. The electrostatic charge effects on the samples were compensated by means of the low-energy electron source working in combination with a magnetic immersion lens. The carbon C1s line with position at 284.6 eV was used as a reference to correct the charging effect. The surface atomic concentration of the elements was determined from peak areas using the appropriate sensitivity factors26. Spectrum background was subtracted according to Shirley27. The XPS spectra of the TiO2 and Cu-species were deconvoluted by way of the CasaXPS-Vision 2, Kratos Analytical UK.

Atomic Force Microscopy (AFM) and Contact Angle Measurements (CA). The atomic force microscopy to characterize the surface morphology was investigated using an UHV-VT-SPM Omicron unit working in noncontact mode (needle sensor). The contact angles (CA) quantifying the hydrophobicity of the cotton samples as a function of sputtering time were assessed by means of a DataPhysics OCA 35 unit following the sessile method for water droplets.

Inductively Coupled Plasma Spectrometry (ICPS). This technique was used to determine the Cu and Ti since it is a sensitive analytical technique due to the low background and high ion-transmission. The Finnigan^{TM} instrument used was equipped with a double focusing reverse geometry mass spectrometer capable of a spectral signal resolution of 1.2 × 10^5 cps/ppb, detection limit of 0.2 ng/L. Samples of 1 cm^2 were placed in Eppendorf tubes containing 1 mL of NaCl/KCl 0.08% solution. The solutions were then diluted 10 times to reach the volume necessary for the ICPS analysis.

X-ray Diffraction of Samples (XRD). The identification of the TiO_2 crystallographic phases and Cu characteristic peaks was carried out by means of an X'Pert diffractometer of the Philips, Delft, NL. The Kα line of Cu (1.5409 Angströms) radiation was used to reference the peaks found.

RESULTS AND DISCUSSION

About the Bacterial Inactivation Kinetics by TiO_2/Cu Samples. Samples of TiO_2/Cu in the dark in Figure 2a sputtered for different times led to *E. coli* inactivation. Figure 2 shows that the sample sputtered with TiO_2 for 10 min followed by sputtering Cu for 40 s (from now on TiO_2/Cu (10 min/40s)) led to the fastest bacterial inactivation. This time is much shorter compared to the inactivation time by Cu-cotton samples inactivating a similar concentration of bacteria within 120 min as reported previously by our laboratory.[17] Table 1 shows that a loading of 0.130 wt % Cu/wt cotton is sputtered within 40 s on 10 min TiO_2 sputtered layers on cotton. Cu sputtered within 40 s on cotton alone led to a value of 0.230 wt % Cu/wt cotton. This implies a lower surface Cu-dispersion. The later samples led to longer inactivation times (data not shown, see ref 17). Cu sputtering on cotton within 40s seems to produce the most suitable structure−reactivity relation for Cu-nanoparticles attaining the best exposure for the Cu-sites to interact with *E. coli*.

Figure 2b presents the results for the TiO_2/Cu (10 min/40s) sample under low intensity visible actinic light inactivating bacteria within <5 min (Figure 2b, trace 4). The actinic light source is shown in the inset to Figure 2b. The bacterial inactivation proceeds faster on TiO_2/Cu samples compared to Cu-samples as recently reported by our laboratory.[17] The fast kinetic inactivation by TiO_2/Cu samples (Figure 2b) provides a further proof for the additional effect of TiO_2 photocatalysis damaging the functional groups of the cell-wall envelope. These damages that facilitate the transport of the Cu-ions through the cell wall have been recently reported.[10,24,25]

DRS of TiO_2/Cu Samples and Some Comments on the Interfacial Reaction Mechanism. Figure 3 shows the results for the diffuse reflection spectroscopy (DRS) for the TiO_2/Cu films sputtered 10 min for TiO_2 and at different times for Cu. The increase in the spectra in Kubelka−Munk units with the Cu-sputtering time is shown in Figure 3. Longer Cu-sputtering times led to shorter bacterial inactivation times (see Figure 2b). The Cu-absorption spectra between 530 and 570 nm has been reported.[28] The DRS spectra of the TiO_2/Cu-films in Figure 3 are very similar to the spectra reported by Bard for CuO.[29]

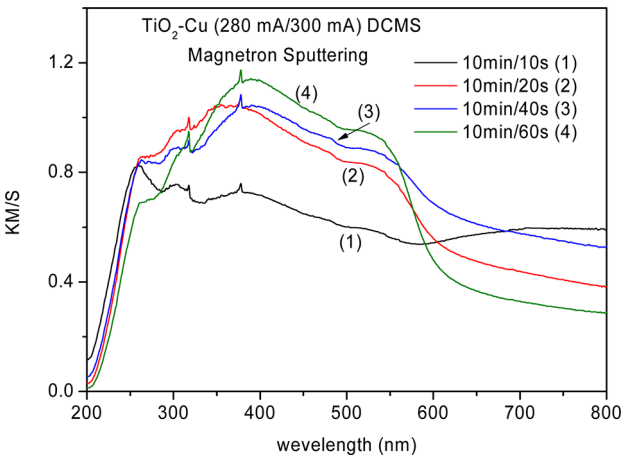

Figure 3. Diffuse reflection spectra of TiO_2/Cu sputtered on cotton for different times plotted in Kubelka−Munk units.

The Cu/TiO_2 absorption in the 700−800 nm region is due to the to the Cu(II) transition.[11,27] The Cu-spectra in Figure 3 shows that Cu was not incorporated into the TiO_2 lattice structure but was only deposited on its surface.

The irradiation of the TiO_2/Cu samples under 400 and 700 nm light (Figure 2b) involves (a) interfacial charge transfer (IFCT) from the valence band TiO_2vb to Cu(II),[11,31,32] and

dx.doi.org/10.1021/am301153j | ACS Appl. Mater. Interfaces 2012, 4, 5234−5240

(b) the formation of Cu Plasmon band.[29] Another factor enhancing the electron transfer interfacial kinetics (IFCT) is due to the TiO_2 forming a Schottky contact with Cu.[12,20] The work function of Cu is 4.5 eV higher than the electron affinity of TiO_2 of 3.9 eV. The Cu-species extracts electrons from the TiO_2 and this leads to an increase in the TiO_2 oxidative ability due to the depleted TiO_2 layer.

The reaction of Cu(II) with O_2 leads to H_2O_2 through a 2 electron reduction: $2Cu(I) + O_2 + 2H^+ \rightarrow 2Cu(II) + H_2O_2$[21,33] or a 4 electron reduction: $4Cu(I) + O_2 + 4H^+ \rightarrow 4Cu(II) + 2H_2O$.[21,33] The reduction of O_2 seems possible due to the potential Cu(II)Cu(I) E^o =0.16 V(SHE, pH 0). Yu and Ran[32] have recently reported that the potential of Cu(II)/Cu is lower than TiO_2 favoring the electron transfer from the conduction band TiO_2cb to Cu(II). The electrons transfer through a multielectron reduction mechanism.[11,30,31]

Visual Appearance of Sputtered Samples. The visual appearance of sputtered cotton samples is shown in Figure 4.

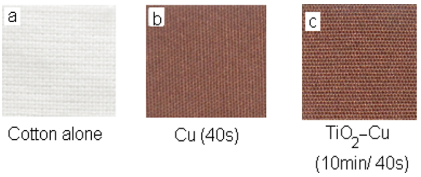

Figure 4. a) Cotton alone, b) DC-sputtered films of Cu on cotton for 40s and c) TiO_2/Cu (10 min-40 s) on cotton.

The brown color becomes darker when Cu is sputtered for similar times on TiO_2 layers as shown in Figure 4c). The brown color corresponds to Cu/Cu_2O with a band gap of 1.7 eV, a flat-band potential of −0.3 V SCE (pH 7), and a valence band at +1.4 V SCE and an absorption edge of ~670 nm as reported elsewhere.[33] The CuO (p-type) is a material with a band gap of 1.7 eV, a flat-band potential of −0.3 V SCE (pH 7), and a valence band at +1.4 V SCE.

ICPS Determination of Cu-Ions During Bacteria Inactivation. Figure 5a shows the repetitive release of Cu-ions up to the eighth recycling for diverse TiO_2/Cu samples after each irradiation cycle irradiated by a Lumilux 18W/827 lamp, 4 mW/cm^2. The release of Cu-ions at a level 5−6 ppb from the film TiO_2/Cu (10 min/40s) led to bacterial inactivation as shown in Figure 5a in the (8th cycle). Figure 5a show that thicker TiO_2 layers release Cu-ions reaching lower concentrations able to cause bacterial inactivation at a level of 5−15 ppb/cm^2. Small amounts of Cu are considered not to be cytotoxic[13,34] and their action would take place through the oligodynamic effect. The Cu-ions bind S, N, and COO^- electron donor negative groups of the cell wall entering the bacteria cytoplasma.[35] Free copper causes toxicity, as it generates reactive oxygen species such as superoxide, hydrogen peroxide and the hydroxyl radical. These damage proteins, lipids and DNA.[36] The U.S. Environmental Protection Agency's Maximum Contaminate Level (MCL) in drinking water is 1.3 mg per liter.[37] Copper and copper alloys such as brass have been found to be toxic to bacteria via the oligodynamic effect. The oligodynamic effect is observed in Figure 5a because the rapid disinfection cycles with the sputtered TiO_2/Cu (10 min/ 40 s) cotton samples released after 8 cycles 20 ppb/cm^2 of Cu well below standards established for cytotoxicity for a variety of living organisms.[38]

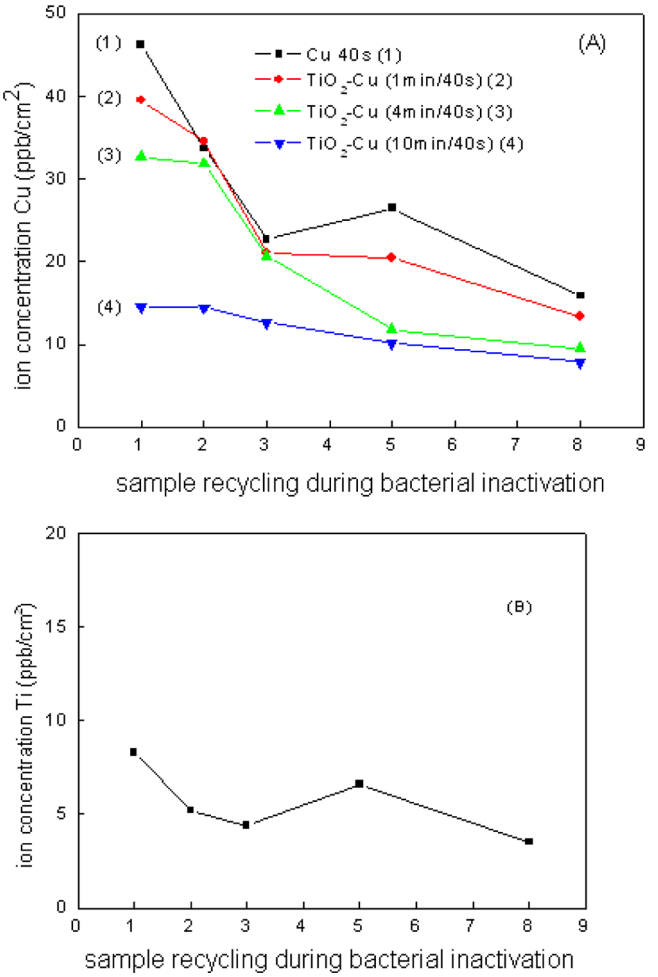

Figure 5. (a) Cu ions release fron diverse Cu-cotton and TiO_2/Cu cotton-sputtered films as a function of catalyst cyclings up to the 8th cycle. (b) Ti- ions release fron diverse TiO_2/Cu (10 min/40 s) cotton-sputtered sample as a function of catalyst cyclings up to the 8th cycle.

A lower release of Ti ions starting with 8 ppb Ti ions and decreasing to 4 ppb after the eighth repetitive recycling is shown in Figure 5b. The low level release of Ti ions is consistent with the high stability known for TiO_2.

Electron Microscopy of TiO_2/Cu Samples (TEM). Figure 6a presents the ultramicrotome cut at 37° of the sample in contact with the enrobing epoxide polymer. Figure 6b shows the sample sputtered for 10 min with a semicontinuous/ compact TiO_2 layer ~40−50 nm wide. Figure 6c presents the TiO_2/Cu (10 min/40 s) sample with lower density gray film TiO_2 ~50 nm wide interdispersed with a more dense darker upper Cu layer. As the TiO_2 layer thickness increased, the composite interdispersed layer became darker suggesting a more compact microstructure.

Atomic Force Microscopy (AFM). Figure 7a shows the AFM image of a TiO_2/Cu (10 min/40 s) on Si wafers taken on a 600 × 600 nm surface. The surface microstructure exhibits a uniform grain distribution with an average size of 30 nm and a root-mean-square roughness (rms) of 1.8 nm. Figure 7b shows the AFM image for the TiO_2/Cu (1 min/40 s) film deposited on Si-wafers. The surface microstructure consisted of grains ~40−60 nm in diameter composed of smaller crystallites with 15−20 nm average size with an rms values of 2.2 nm. The size of the grains became bigger in the case of the TiO_2 1 min

dx.doi.org/10.1021/am301153j | ACS Appl. Mater. Interfaces 2012, 4, 5234−5240

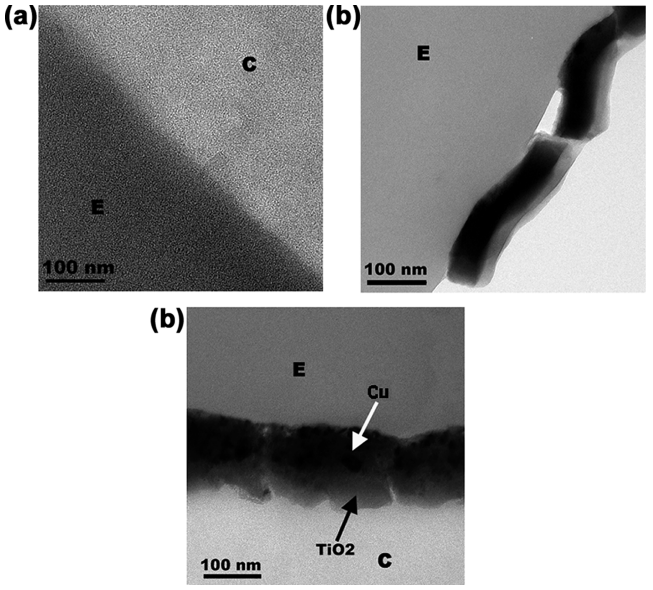

Figure 6. TEM of (a) a cotton sample alone (C, cotton; E, epoxide), (b) TiO_2-sputtered cotton sample for 10 min, (c) DC-sputtered cotton sample TiO_2/Cu (10 min/40 s).

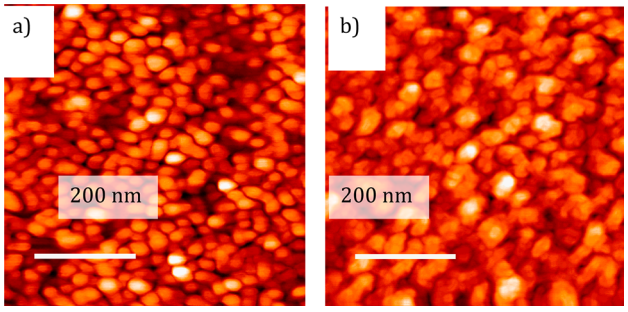

Figure 7. AFM images of: (a) TiO_2/Cu (10 min/40 s) DC-magnetron sputtered samples and . (b) TiO_2/Cu (1 min/40 s) samples.

sputtered samples compared to the 10 min TiO_2 samples. This leads to films presenting a higher rugosity.

Contact Angle Measurements (CA). Figure 8a, shows an initial contact angle of 81° for Cu cotton samples sputtered for 40s. This angle decreases to 8° after 60s indicating that the water droplet penetrates the Cu cotton. An increase in hydrophobicity is shown in Figure 8b for TiO_2/Cu (10 min/40s) samples showing an initial contact angle of 105°. The adsorption of the water droplet slows down compared to Figure 8a because the void area in the cotton further decreases due to the sputtered TiO_2 layers. The roughness values for both samples (<2.5 nm) is small, hence it is unlikely that roughness will significantly influence the CA-measurements.

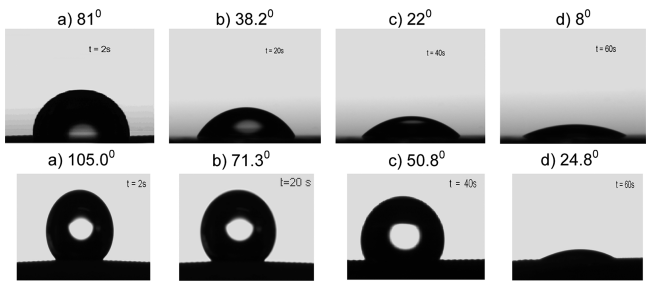

Figure 8. (a) Contact angle (CA) of a water droplet on cotton-sputtered 40 s with Cu as a function of time. (b) Contact angle (CA) of a water droplet on cotton sputtered TiO_2/Cu 10 min/40 s) as a function of time.

XPS Analyses of the Samples During Bacterial Inactivation. Table 2 shows the surface atomic composition at time zero for cotton, cotton TiO_2 sputtered for 10 min, cotton Cu sputtered for 40 s and TiO_2/Cu(10 min/40 s) films. It is readily seen that the TiO_2/Cu (10 min/40 s) film has the same surface Cu atomic concentration as Cu-cotton sputtered for 40 s. Therefore, the microstructure of the Cu-nanoparticulate topmost layers are modified significantly by TiO_2, because the bacterial inactivation by the TiO_2/Cu film in Figure 2b shows bacterial inactivation within 5 min compared to 60 min as recently reported.[18]

Table 2. Surface Atomic Percentage Concentration of Cu for Different Sputtered Films

sample	C	O	N	Cu	Ti
cotton alone	71.22	25.24	0.54	0	0
TiO_2 (10 min)	28.51	51.23	0.36	0	19.90
Cu (40 s)	50.38	19.49	0.48	29.65	0
TiO_2/Cu(10 min/40 s)	48.47	19.72	0.43	31.39	0

The fast catalysis at the surface of the catalyst led the self-cleaning action of the C, O and N bacterial decomposition residues. This is shown in Tables 3. No accumulation of C, O, and N takes place during the bacterial inactivation time.

Table 3. Surface Atomic % Concentration of Cotton-Sputtered Samples TiO_2/Cu (10 min/40 s) during *E. coli* Inactivation

sample identifier	C	O	N	Cu
zero s	41.54	28.48	0.36	29.62
3 s	58.63	34.27	1.09	6.02
5 min	63.41	34.59	0.58	1.42

The C contamination of the sample is due in part to adventitious hydrocarbons adsorbed spontaneously from the ambient air in the room. The C value after the initial increase stabilizes because of the conversion of the C residues to CO_2 on the catalyst surface. The decrease in the Cu(I) species during bacterial inactivation and the concomitant growth of Cu(II) describes the redox catalysis taking place in the samples as shown in Table 4.

Table 4. Surface Atomic Concentration Percentage of TiO_2/Cu (10 min/40s) during *E. coli* Inactivation

time	Cu/Cu_2O %	CuO %
zero sec	65.35	34.65
3 s (bacteria)	9.53	90.47
5 min (bacteria)	1.88	98.12

Figure 9a presents the spectrum of the Cu2p doublet with the shakeup satellites (also labeled vibrational satellites) of CuO at 934.5 eV and of Cu_2O at 932.4 eV.[39] Figure 9a and Table 4 show that for the TiO_2/Cu (10 min/40s) film at time zero, the majority of Cu exists as Cu/Cu_2O (63.35%) with a CuO content of 34.65%. Exposure of this sample to the bacterial suspension for the 3s results in a strong oxidation of

dx.doi.org/10.1021/am301153j | ACS Appl. Mater. Interfaces 2012, 4, 5234−5240

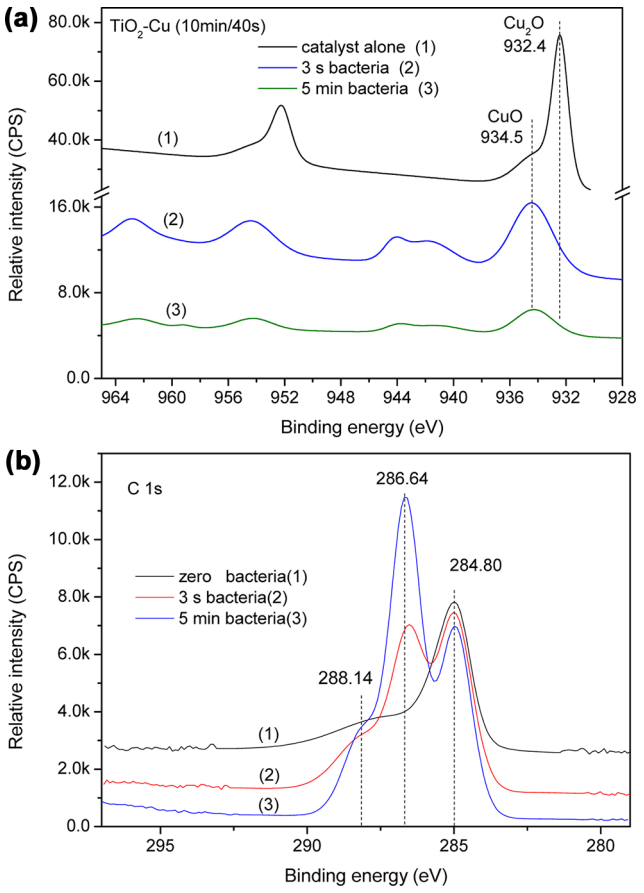

Figure 9. (a) XPS Cu2p doublet and the shake up satellites representing CuO at 934.5 eV and Cu_2O at 923.3 eV of a TiO_2/Cu (10 min/40 s) film: (1) time zero, (2) film contacted with bacteria for 3 s, and (3) after 5 min bacterial inactivation reaction under low-intensity Osram 18W/827 light. (b) XPS signals osf a TiO_2/Cu (10 min/40s) sample as a function of bacterial inactivation time under irradiation by an Osram18W/827 lamp. Relevant peaks: aromatic C−C 284.80 eV, C−O 286.64 eV, and O−C═O 288.64 eV.

the Cu_2O to CuO (90.47%) with a concomitant decrease in the Cu/Cu_2O species to 9.53%. The shakeup satellite bands due to paramagnetic Cu^+ are seen in Figure 9a to decrease with time, which is further confirmed by the data reported in Table 4. The results presented in Figure 9a and Table 4 describe the variation of the Cu^+ and Cu^{2+} as a function of the bacterial inactivation time and are due to the redox catalysis taking place when the Cu layers get in contact with *E. coli*.

When the TiO_2/Cu is irradiated, the TiO_2 can reduce the Cu^{2+} by the TiO_2cb electrons. The redox mechanism implies also reactions oxidizing the Cu^o to Cu ions by the TiO_2vb holes. The Cu on the TiO_2 act as an electron sink and led to a more effective spatial charge reflected in the faster inactivation kinetics. The XPS data shown in Figure 9a and Table 4 provides the evidence for conduction band electrons (cb) reducing Ti^{4+} or Cu^{2+} (CuO) and the valence band holes oxidize O_2^- to O^-, a highly oxidative radical. The electron−hole recombination for Ti^{3+} or Cu^+ with O^- proceeds in parallel to the generation of the highly oxidative radicals.

Figure 9b shows the variation of the XPS C1s signals for the TiO_2/Cu (10 min/40 s) film up to 5 min. The XPS C1s signals are assigned to: (a) C−C aromatic at 284.80 eV, C−O at 286.64 eV, and O−C═O at 288.14 eV. The 286.64 eV peak appears after the film was contacted for 3s with bacteria indicating the formation of oxidative residues during the bacterial inactivation. The peak at 286.64 eV increases after 5 min suggesting additional oxidative functionalities. A small shoulder at 288.14 eV after 5 min is assigned to the O−C═O species. During the course of *E. coli* inactivation, the C1s line shows a different ratio between the carbon component at 286.64 and 288.14 eV. This suggests a complex reaction mechanism during *E. coli* inactivation/oxidation.

X-ray Diffraction (XRD) of TiO_2/Cu Samples. Signals for anatase at 25.2° and weak rutile signals at 27.5° were registered in the XRD spectrogram. No peak at 40° was observed for Cu due to the small quantity of crystalline Cu available on the sputtered films. A strong peak signal at 22.5° was observed originating from the cotton.

CONCLUSIONS

In this study, we have shown the possibility of using low cost Cu/Cu-ions nanoparticulate to substitute noble metals in the fabrication of antibacterial films. Innovative and effective TiO_2/Cu bifunctional films showing fast bacterial inactivation in the dark and under low intensity visible/actinic light were fully characterized during this study. Higher amounts of Cu-sputtered on cotton led to an increase in the spectral absorption of the sputtered films. But increasing the Cu-amount deposited on cotton as determined by XRF, did not significantly increase the bacterial inactivation kinetics, showing that the bacterial inactivation is due to the surface Cu-ions. Evidence is presented that TiO_2 in contact with Cu layers transfers the photoinduced charges to the surface Cu ions by photoinduced IFTC. A relatively low quantity of Cu-ions was able to induce bactericidal inactivation and at levels is not considered cytotoxic. An oligodynamic effect is shown to lead to bacterial inactivation. TiO_2/Cu layers reduce water penetration in the void areas of the cotton fabrics increasing the hydrophobicity of the cotton surface. This is shown to favor the Cu species grafting on the more hydrophobic surfaces.

AUTHOR INFORMATION

Corresponding Author

*E-mail: cessar.pulgarin@epfl.ch (C.P.), john.kiwi@epfl.ch (J.K.).

Notes

The authors declare no competing financial interest.

ACKNOWLEDGMENTS

We thank the COST Action MP0804 Highly Ionized Impulse Plasma Processes (HIPIMS), COST action TD0906:Biological Adhesives: from biology to biomimetics and the EPFL for support of this work.

REFERENCES

(1) Page, K.; Wilson, M.; Parkin, P. I. *J. Mater. Chem.* **2009**, *19*, 3819−3831 and references therein..

(2) Page, K.; Palgrave, R.; Parkin, P. I.; Wilson, M.; Shelley, S.; Chadwick, A *J. Mater. Chem.* **2007**, *17*, 95−104.

(3) Scholz, J.; Nocke, G.; Hollstein, F.; Weissbach, A *Surf. Coat. Technol.* **2005**, *192*, 252−256.

(4) Foster, H. A.; Sheel, W. D.; Sheel, P.; Evans, P; Varghese, S.; Rutschke, N.; Yates, M. H. *J. Photochem. Photobiol. A.* **2010**, *216*, 283−289.

(5) Dunlop, M. S. P.; Sheeran, P. C.; Byrne, A. J.; McMahon, S. A. M; Boyle, A. M.; McGuigan, G. K. *J. Photochem. Photobiol. A.* **2010**, *216*, 303−3010.

(6) Borkow, G.; Gabbay, J. *Med. Hypothesis* **2008**, *70*, 990−994.
(7) Borkow, G.; Gabbay, J. *J. FASEB* **2004**, *188*, 1728−1730.
(8) Lin, J.; Moore, J.; Sproul, W.; Mishra, B.; Wu, Z.; Wang. *Surf. Coat. Technol.* **2010**, *204*, 2230−2239.
(9) Sarakinos, K.; Alami, J.; Konstantinidis, D. *Surf. Coat. Technol.* **2010**, *204*, 1661−1684.
(10) Sunada, K.; Watanabe, T.; Hashimoto, K. *Environ. Sci. Technol.* **2003**, *37*, 4785−4789.
(11) Irie, H.; Miura, S.; Kamiya, K.; Hashimoto, K *Chem. Phys. Lett.* **2008**, *457*, 202−205.
(12) Hashimoto, K; Irie, H; Fujishima, A. *J. Appl. Phys.* **2005**, *44*, 8269−8285.
(13) Heidenau, F; Mittelmeier, F.; Detsch, R.; Haenle, M.; Gollwitzer, H. *J. Mater. Sci.: Mater. Med.* **2005**, *16*, 883−888.
(14) Haenle, M.; Fritshe, M.; Zietz, C.; Bader, R.; Heidenau, F. *J. Mater. Sci.: Mater. Med.* **2011**, *22*, v381−387.
(15) Paschoalino, M.; Guedes, C. N.; Jardim, W.; Mielczarski, E.; Mielczarski, J.; Bowen, P.; Kiwi, J *J. Photochem. Photobiol. A* **2008**, *199*, 105−111.
(16) Torres, A.; Ruales, C.; Pulgarin, C.; Aimable, A.; Bowen, P.; Kiwi, J. *ACS Appl. Mater, Interfaces* **2010**, *2*, 2547−2552.
(17) Castro, C.; Sanjines, R.; Pulgarin, C.; Osorio, P.; Giraldo, A.; Kiwi, J. *J. Photochem. Photobiol. A* **2010**, *216*, 295−302.
(18) Osorio, P.; Sanjines, R.; Ruales; Castro, C.; Pulgarin, C.; Rengifo, J-A; Lavanchy, J.-C.; Kiwi, J. *J. Photochem. Photobiol. A.* **2011**, *220*, 70−76.
(19) Ehiasarian, A.; Pulgarin, C.; Kiwi, J. *Env. Sci. Pollut. Res.* **2012**.
(20) Kusiak-Nejman, E.; Morawski, A.; Ehiasarian, P. A.; Pulgarin, C.; Mielczarski, E.; Mielczarski, O.; Baghriche, J.; Kulik, A.; Kiwi, J. *J. Phys. Chem. C* **2011**, *115*, 21113−21119.
(21) Laura, R; Kusiak, E.; Kiwi, J.; Pulgarin, C.; Trampuz, A.; Bizzini, A. *J. Appl. Microbiol.* **2012**, submitted.
(22) Bacsa, R.; Kiwi, J.; Ohno, T.; Albers, P.; Nadtochenko, V. *J. Phys. Chem. B* **2005**, *109*, 5994−6003.
(23) Nadtochenko, V.; Rincon, A.; Stanka, S; Kiwi, J. *J. Photochem. Photobiol. A* **2005**, *169*, 131−137.
(24) Kiwi, J.; Nadtochenko, V. *J. Phys. Chem. B* **2004**, *108*, 17675−17684.
(25) Kiwi, J.; Nadtochenko, V. *Langmuir* **2005**, *21*, 4631−4641.
(26) Shirley, D. A *Phys. Revs* **1972**, *B5*, 4709−4716.
(27) Fujishima, A.; Tao, T.; Tryk, D.; Photocatalytic, D. *J. Photochem. Photobiol. C* **2000**, *1*, 1−21.
(28) Hardee, K.; Bard, A. *J. Electrochem. Soc.* **1977**, *125*, 215−224.
(29) Henglein, A. *J. Phys. Chem.* **2000**, *104*, 1206−1211.
(30) Qiu, X.; Miyauchi, M.; Yu, H.; Irie, H.; Hashimoto, K *J. Am. Chem. Soc.* **2010**, *132*, 15259−15263.
(31) Zhang, J.; Yu, J.; Zhang, Y.; Li, Q.; Gong, J. *Nano Lett.* **2011**, *11*, 4774−4779.
(32) Yu, J; Ran, J *Energy Environ. Sci.* **2011**, *4*, 1364−1371.
(33) Bandara, J.; Guasaquillo, I.; Bowen, P.; Soare, L; Jardim, W.; Kiwi, J. *Langmuir* **2005**, *21*, 8554−8559.
(34) Thüringer Surface and Biomaterials Kolloquium, 13/15 September 2011, Zeulenroda, Germany.
(35) Ewald, A.; Glükermann, S.; Thull, R.; Gburek, U. *Res. Biomed. Eng.* **2005**, 22−26.
(36) Brewer, G. J. *Clin. Neurophys.* **2010**, *121*, 459−60.
(37) Casarett, E & Doull's, S. *Toxicology, The Basic Science of Poisons*, fifth ed.; Klassen, C. D., Ed.; McGraw-Hill: New York, 2000; p 715.
(38) Prociv, P. *Med. J. Aust* **2004**, *181*, 344−352.
(39) Wagner, D. C.; Riggs, W. M.; Davis, L. E.; Mullenberg, E. G. *Handbook of X-Ray Photoelectron Spectroscopy*; Perkin-Elmer Corp, Physical Electronics Division;, Eden Prairie, MN, 1979.